BELLE2-NOTE-PL-2020-014
July 24, 2020

Measurement of the tracking efficiency and fake rate with $e^+e^- \to \tau^+\tau^-$ events

The Belle II Collaboration

Abstract

The tracking efficiency and fake rate have been measured using $e^+e^- \to \tau^+\tau^-$ events, where one tau lepton decays leptonically ($\tau \to \ell^{\pm}\nu_\ell\bar{\nu_\tau}$, $\ell = e,\ \mu$) while the other decays hadronically into three charged pions ($\tau \to 3\pi^{\pm}\nu_\tau + n\pi^0$). These measurements were performed using the e^+e^- collision data recorded during the 2019a, 2019b and 2019c data taking periods. This document contains the approved plots and captions.

Contents

1. TRIGGER

In order to measure the efficiency of the ECL triggers in data, orthogonal CDC triggers are used as a reference:

$$\epsilon_{hie} = \frac{\text{(ffo or fff) and hie}}{\text{(ffo or fff)}} \ , \qquad \epsilon_{lml0} = \frac{\text{(ffo or fff) and lml0}}{\text{(ffo or fff)}} \ , \tag{1}$$

where the ECL triggers require:

- *hie* : total ECL energy above 1 GeV, and not an ECL Bhabha.
- *lml0* : at least 3 ECL clusters, energy of at least one of the clusters above 300 MeV, and not an ECL Bhabha.

and the reference triggers require:

- *ffo* : at least two CDC tracks with $\Delta\phi > 90°$, and not an ECL Bhabha.
- *fff* : at least three CDC tracks.

Figures 1 and 2 shows the measured ECL trigger efficiency in data as defined in equation 1, respectively for the electron and muon channel.

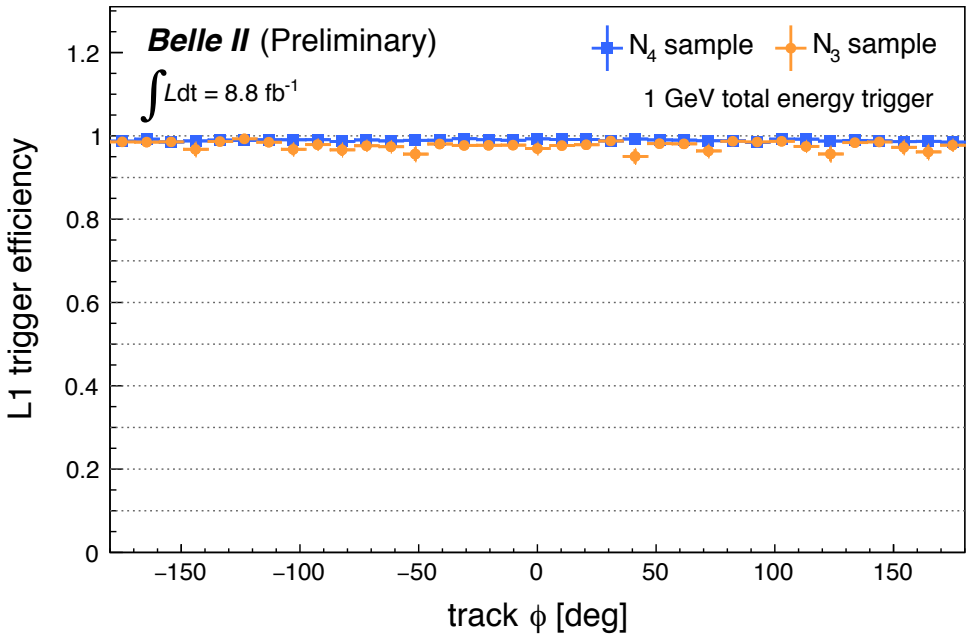

FIG. 1: The *hie* trigger efficiency in the electron channel measured as a function of the 1-prong track ϕ in the combined 2019a, 2019b and 2019c data. The efficiency in the 4- and 3-track sample is shown in blue and orange, respectively. Statistical uncertainties are shown.

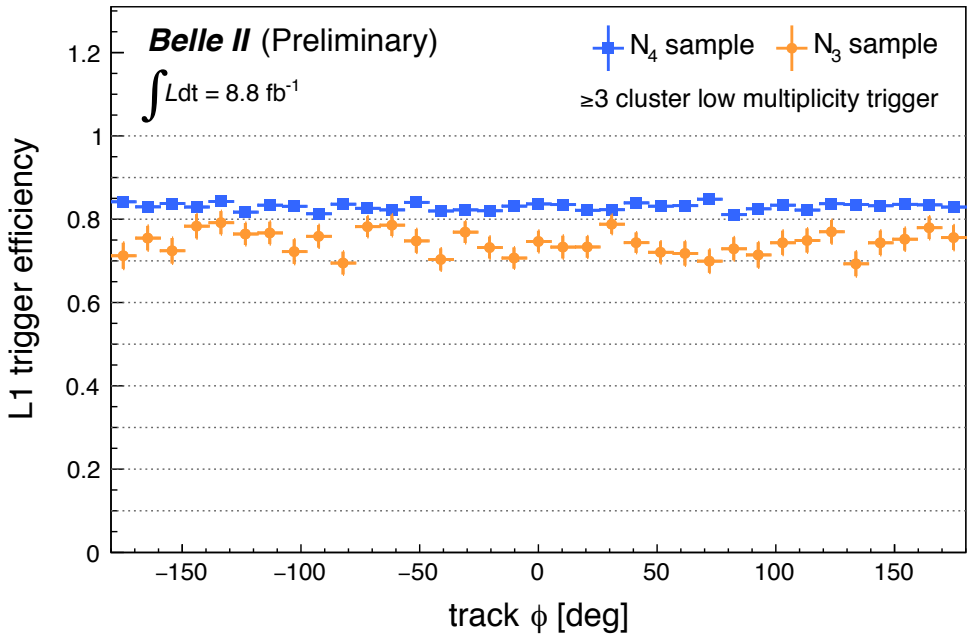

FIG. 2: The *lml0* trigger efficiency in the muon channel measured as a function of the 1-prong track ϕ in the combined 2019a, 2019b and 2019c data. The efficiency in the 4- and 3-track sample is shown in blue and orange, respectively. Statistical uncertainties are shown.

2. BACKGROUND SUPPRESSION

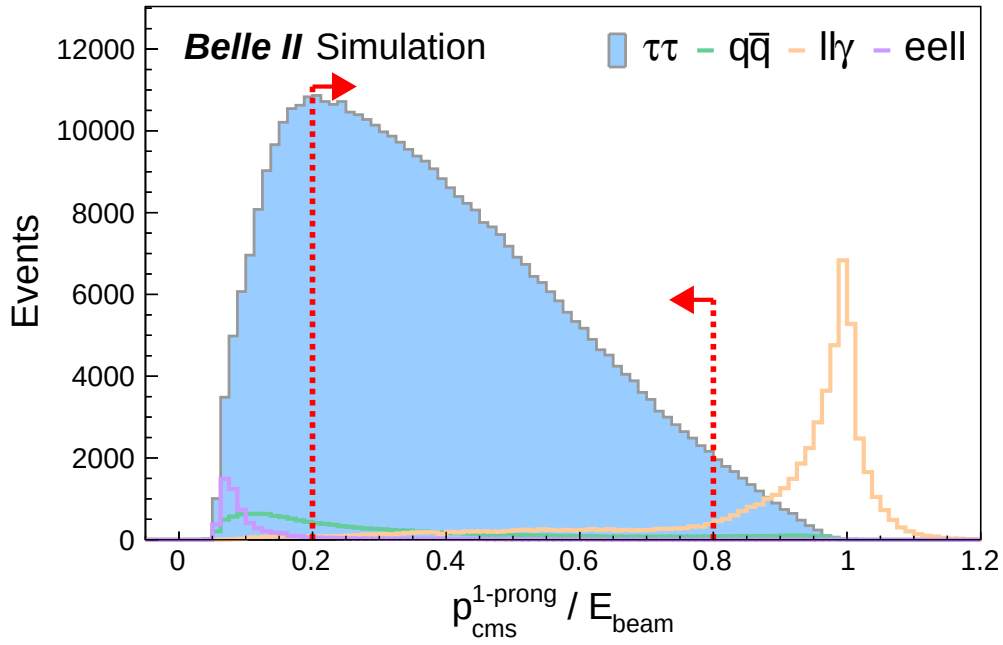

FIG. 3: Distribution in MC simulation of the 1-prong track momentum in the CMS frame divided by the beam energy. The red arrows indicates the cut values.

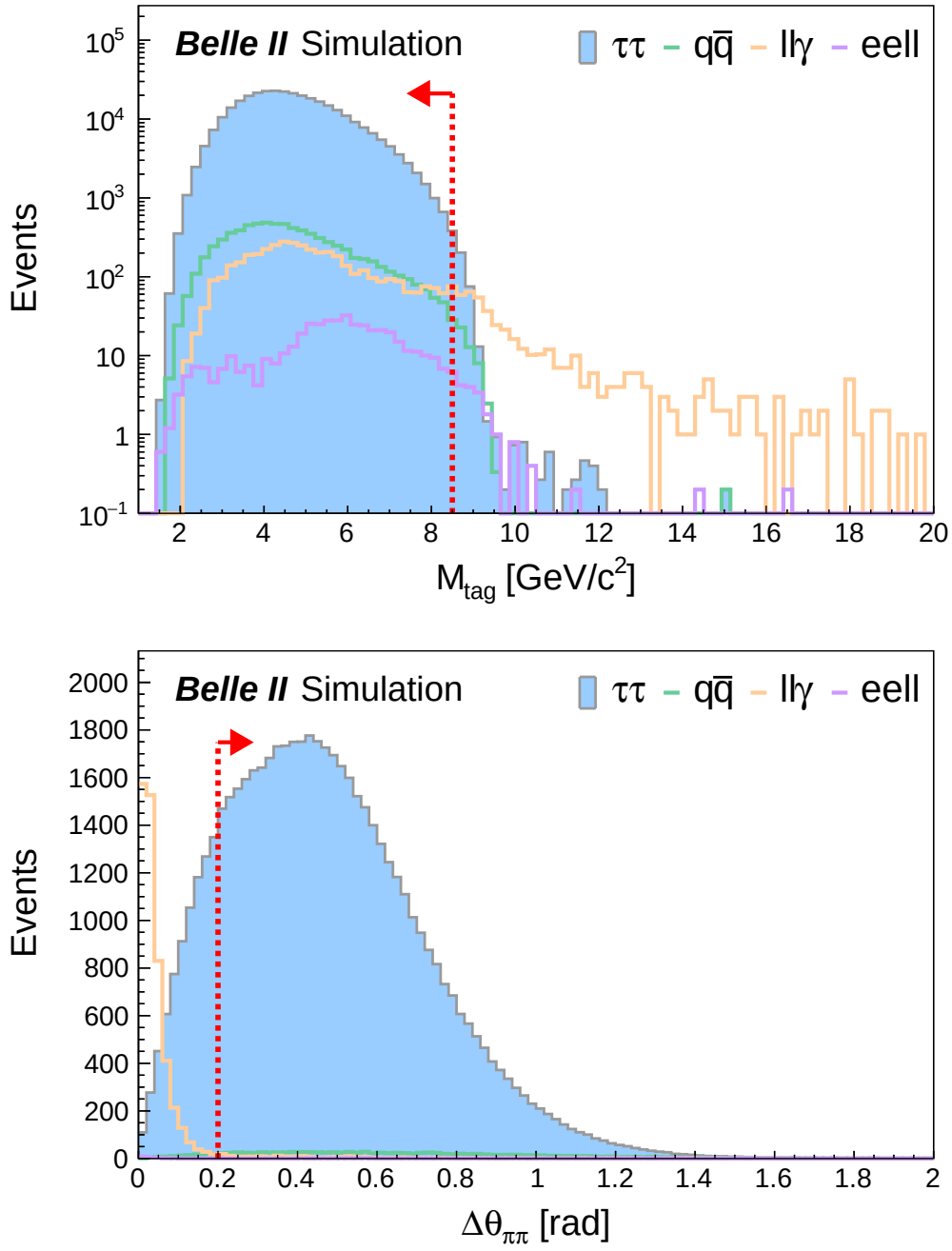

FIG. 4: Distributions in MC simulation of the invariant mass of the three tag-track candidates M_{tag} (top) and the 2-prong opening angle for the electron channel (bottom). The red arrows indicates the cut values.

3. DATA-MC COMPARISON

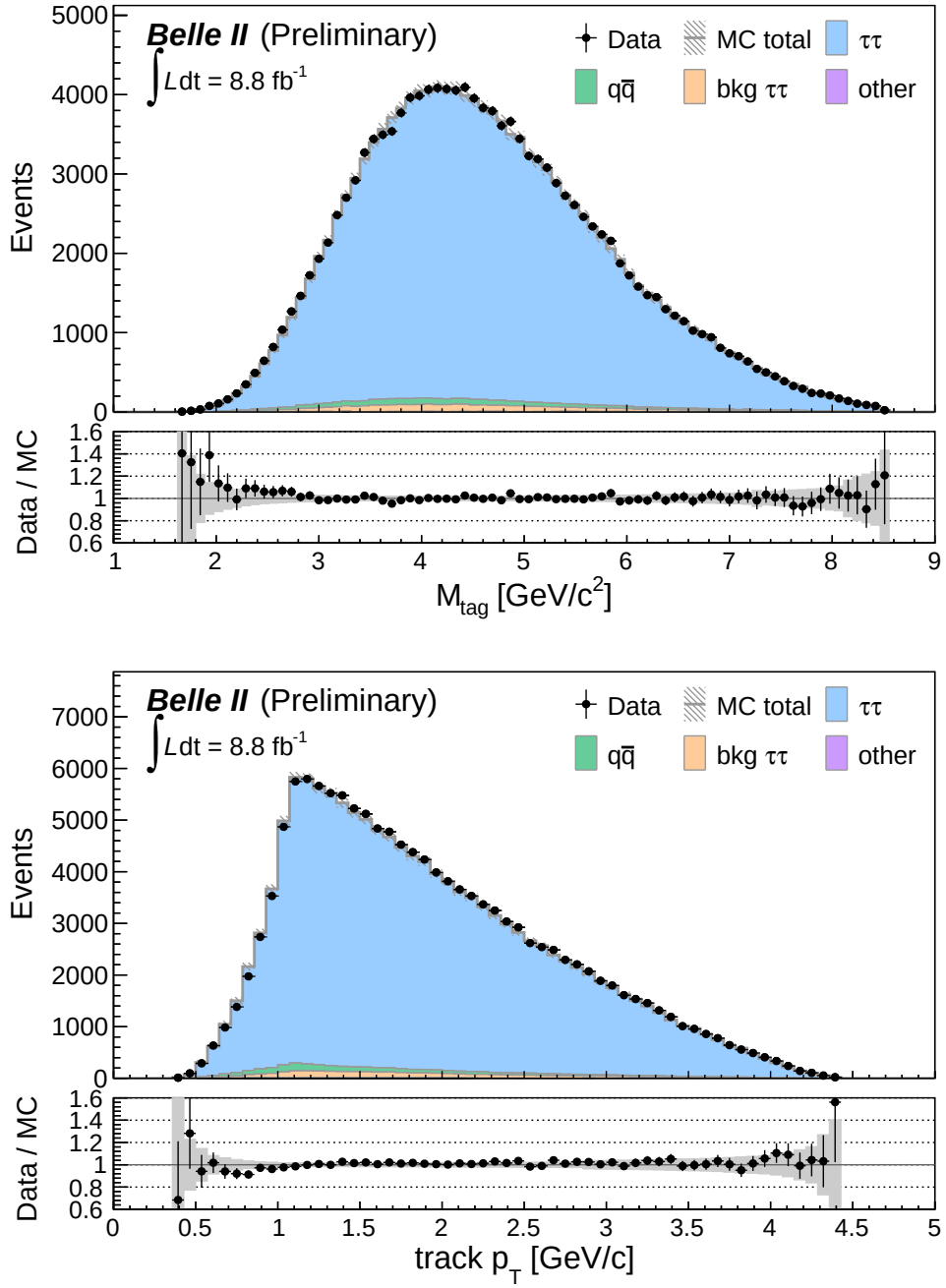

FIG. 5: Distributions in the combined 3- and 4-track samples (all channels and charges) of the invariant mass of the three tag-track candidates M_{tag} (top) and 1-prong track p_T (bottom). The data (points) are compared to the signal + background expectation (stacked histograms). Statistical uncertainties for Data and MC are shown, with the MC error band including also the trigger efficiency uncertainty. The lower panel shows the Data/MC ratio.

4. CALIBRATION OF THE EFFICIENCY ESTIMATOR

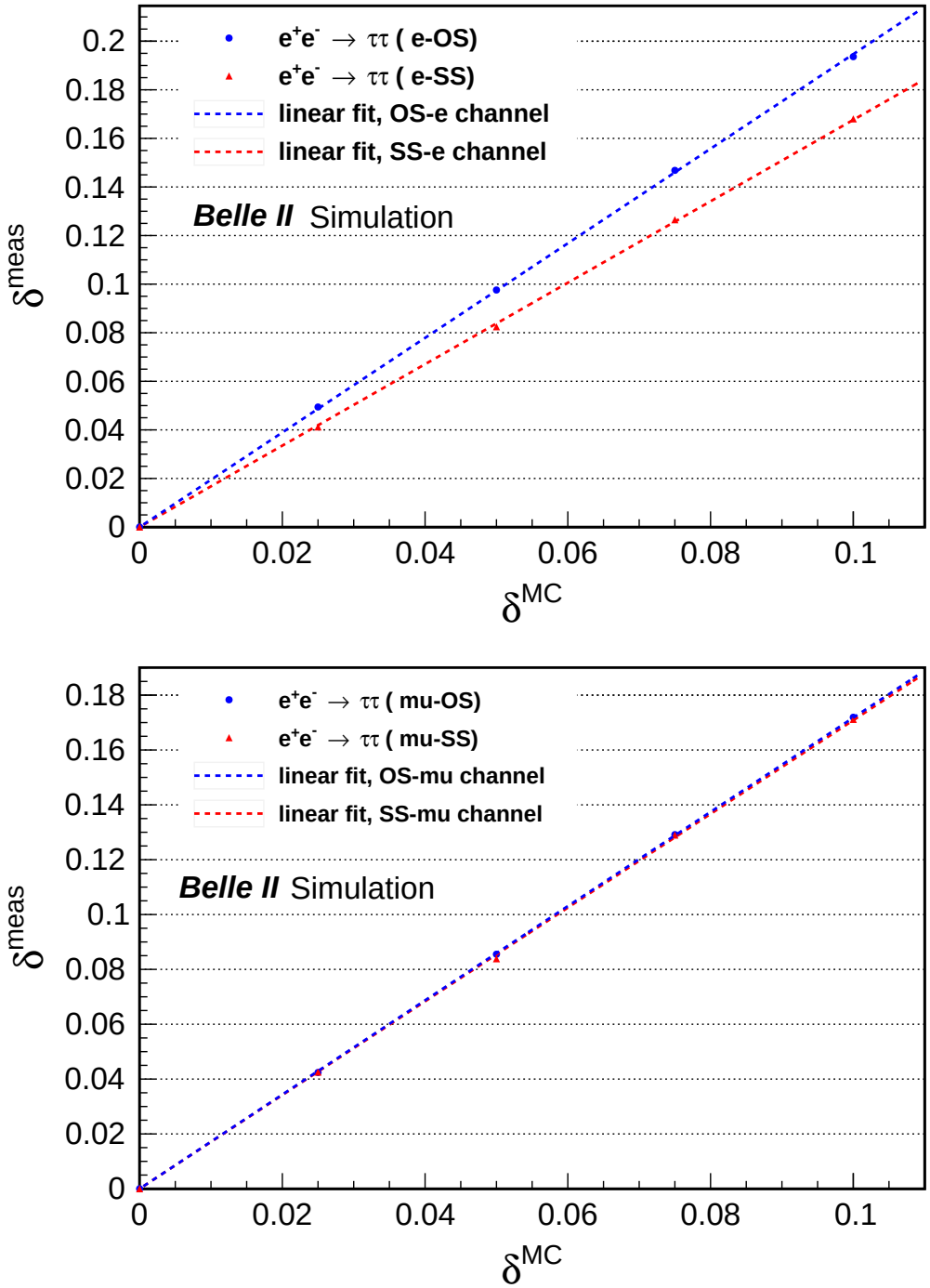

FIG. 6: Calibration curves showing the measured discrepancy δ^{meas} as a function of the true one, δ_{MC}, for the electron (top) and muon (bottom) channels and for both charges OS (blue) and SS (red). The fit results provide the calibration curve slopes which correspond to the different k-factors: $k_{OS}^{\text{electron}} = 1.95 \pm 0.01$, $k_{SS}^{\text{electron}} = 1.68 \pm 0.01$, $k_{OS}^{\text{muon}} = 1.718 \pm 0.005$, $k_{OS}^{\text{muon}} = 1.709 \pm 0.008$.

5. EFFICIENCY MEASUREMENT

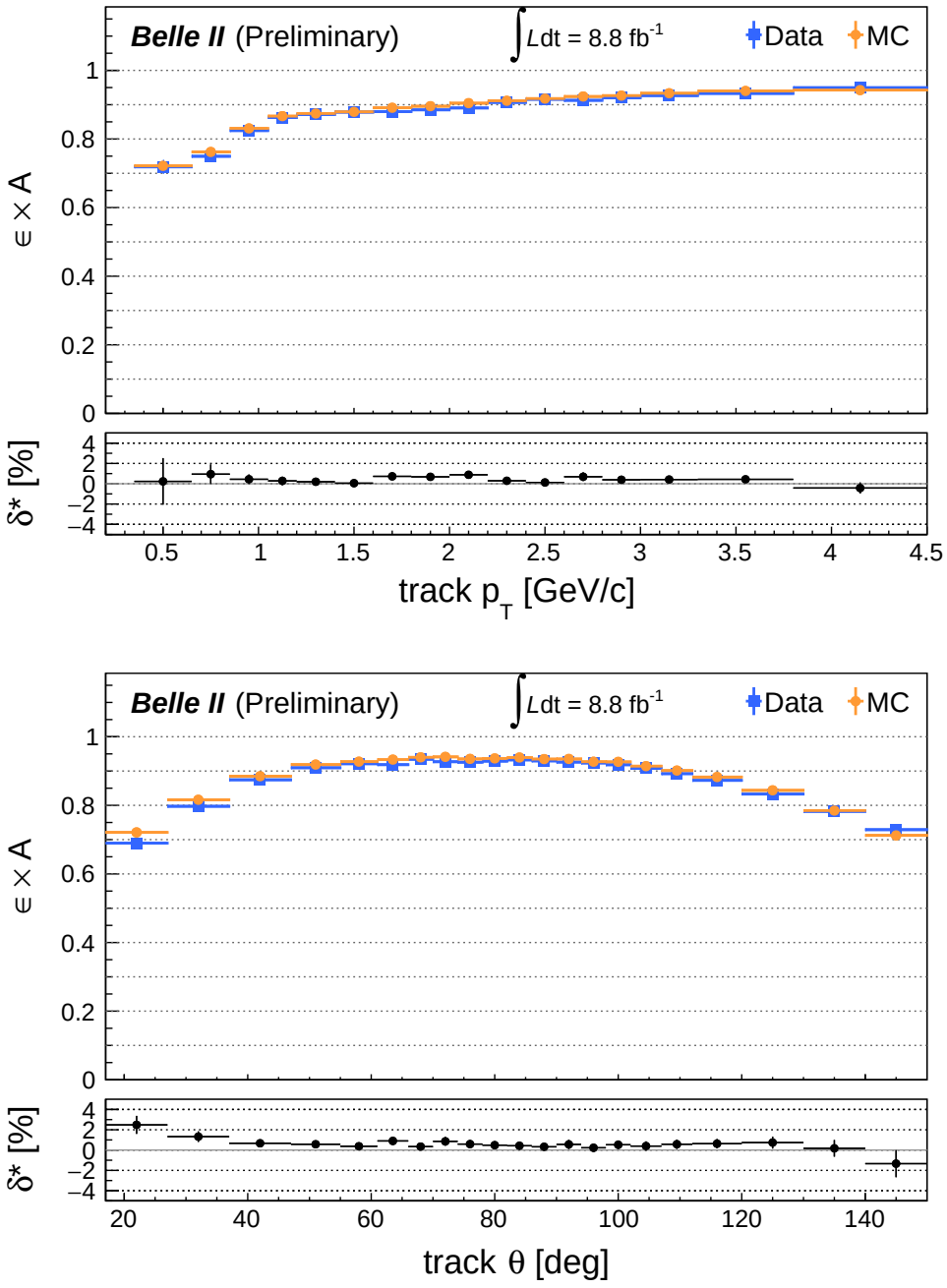

FIG. 7: The measured tracking efficiency times detector acceptance ($\epsilon \times A$) and calibrated Data-MC discrepancy (δ^*) for the combined channels as a function of the 1-prong track p_T (top) and θ (bottom). The upper panel compares $\epsilon \times A$ in data (blue) and MC (orange), while the lower panel shows δ^*. Statistical uncertainties are shown.

6. CALIBRATED DISCREPANCIES

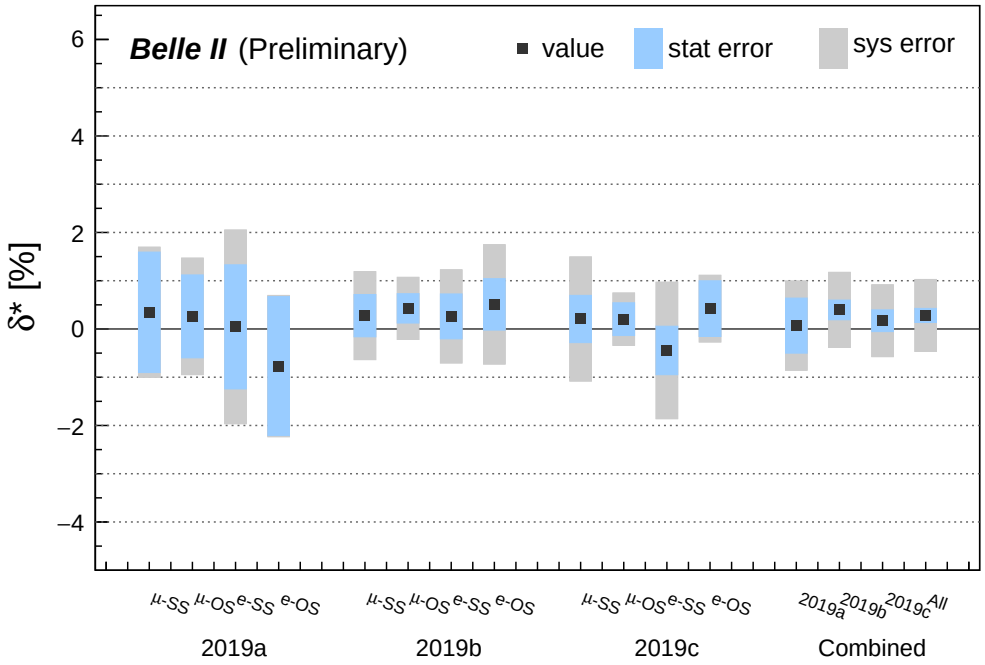

FIG. 8: The overall calibrated Data-MC discrepancy for the tracking efficiency (δ^*). The measurement is shown for the individual channels (μ-SS, μ-OS, e-SS, e-OS) as well as for the different data taking periods (2019a, 2019b, 2019c). The δ^* for the combined channels are shown in the rightmost four bins. Statistical (grey) and total systematic (blue) uncertainties are shown.

7. FAKE RATE MEASUREMENT

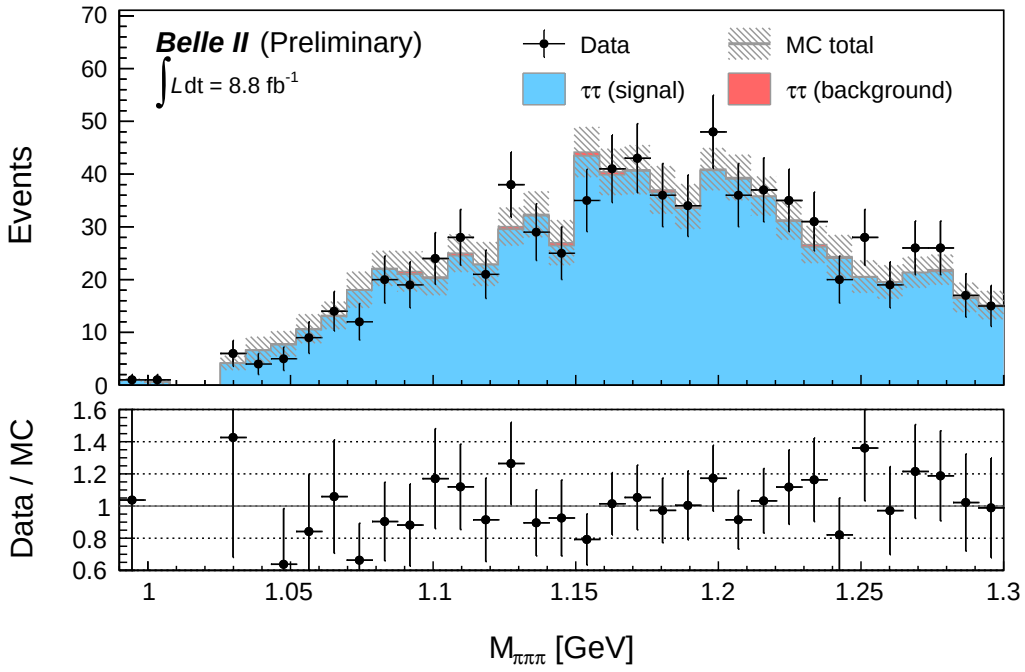

FIG. 9: Distribution in the combined 4- and 5-track samples of the 3-prong invariant mass ($M_{\pi\pi\pi}$). The data (points) are compared to the signal + background expectation (stacked histograms). Statistical uncertainties for Data and MC are shown, with the MC error band including also the trigger efficiency uncertainty. The lower panel shows the Data/MC ratio.

8. CONCLUSION

The *Belle II* track finding efficiency and fake rate have been measured in the 2019 data (2019a, 2019b, 2019c) using tag-and-probe methods targeting $e^+e^- \to \tau^+\tau^-$ events.

When comparing the 2019 data to run independent MC, the overall value of the calibrated data-MC discrepancy for the efficiency is measured to be:

$$\delta^*_{\text{efficiency}} = 0.28 \ \pm \ 0.15 \text{ (stat)} \ \pm \ 0.73 \text{ (sys)} \ \% \ , \tag{2}$$

The tracking fake rate has also been measured in 2019 data. With the help of the signal purities in MC simulation, we give two estimations of the true rate r_{fake} in data (without any background event):

$$r_{\text{fake}} = 0.97 \ \pm \ 0.34 \text{ (stat)} \ \pm \ 0.06 \text{ (sys)} \ \% \ , \tag{3}$$

where the MC signal purity used to estimate the signal yields in data was obtained with the help of the run independent MC samples, and:

$$r_{\text{fake}} = 0.96 \ \pm \ 0.35 \text{ (stat)} \ \pm \ 0.06 \text{ (sys)} \ \% \ , \tag{4}$$

where the run dependent MC samples were used. Both results are compatible with each other within 1σ.